The Structure of the Electric Double Layer: Atomistic vs. Continuum Approaches

Sung Sakong,[1,*] Jun Huang,[1,2] Michael Eikerling,[2] and Axel Groß[1,3,†]

[1]*Institute of Theoretical Chemistry, Ulm University, 89069 Ulm, Germany*

[2]*IEK-13, Forschungszentrum Jülich, Wilhelm-Johnen-Straße, 52425 Jülich, Germany*

[3]*Helmholtz Institute Ulm (HIU), Electrochemical Energy Storage, 89069 Ulm, Germany*

Abstract

This article reviews recent forays in theoretical modeling of the double layer structure at electrode/electrolyte interfaces by current atomistic and continuum approaches. We will briefly discuss progress in both approaches and present a perspective on how to better describe the electric double layer by combining the unique advantages of each method. First-principles atomistic approaches provide the most detailed insights into the electronic and geometric structure of electrode/electrolyte interfaces. However, they are numerically too demanding to allow for a systematic investigation of the electric double layers over a wide range of electrochemical conditions. Yet, they can provide valuable input for continuum approaches that can capture the influence of the electrochemical environment on a larger length and time scale due to their numerical efficiency. However, continuum approaches rely on reliable input parameters. Conversely, continuum methods can provide a preselection of interface structures and conditions to be further studied on the atomistic level.

Keywords: Electric double layer, Semiclassical method, Ab initio molecular dynamics simulations, Electrochemical interfaces

* sung.sakong@uni-ulm.de

† axel.gross@uni-ulm.de

I. INTRODUCTION

Electrochemistry is concerned with structures and processes at interfaces between an electronic conductor, the electrode, and an ionic conductor, the electrolyte [1, 2]. At the interface between a solid electrode and liquid electrolyte, an electric double layer (EDL) is formed by rearranging the electronic and ionic charges under the given electrochemical conditions. The EDL exhibits spatiotemporally fluctuating local polarization due to the liquid nature of electrolytes. Because of the extensive numerical effort associated with the explicit modeling of the atomistic structure, the representative properties of the EDL are usually described by statistically averaged values. One of the most important properties is the electrostatic potential governed by the polarization distribution in the EDL, created by the electronic and ionic charges. Thus, modern EDL theories focus on identifying and modeling the polarization effects, e.g., the orientation of solvent molecules, ion arrangements, and the electron density redistribution [3–10].

Classical approaches typically assume a Boltzmann distribution of the ions in the electrolyte and derive the effective electric potential by solving the Poisson equation. The quality of the methods depends on the aptness and completeness in the description of polarization effects, which are included to varying depths in existing theories. On the one hand, continuum approaches have a long tradition (see, e.g., Ref. [2]), and they continue to be further improved. An example of the ongoing progress made in this field is a recently developed classical model that provides a computationally efficient grand-canonical scheme treating electrode and electrolyte phases on similar footing [7–9]. On the other hand, atomistic approaches based on density functional theory (DFT) accurately evaluate the charge polarization effect and the electrostatic potential for a given atomic configuration. The statistical EDL properties can be sampled along a trajectory using ab initio molecular dynamics (AIMD) simulations [3–6, 10–13] or classical molecular dynamics (CMD) simulations, e.g., with interaction potentials of the Reax force field [14], or deep potential MD, with interatomic forces generated from a deep neural network that is trained with ab initio data [15].

There are various approaches to theoretically model the EDL, ranging from continuum models to DFT-based simulations. In this minireview, we will focus on comparing methods and approaches that can explicitly take the electronic degrees of freedom into account which

is critical for a reliable description of electrochemical interfaces and conditions. We will use selected examples from first-principles atomistic and semiclassical continuum approaches, and we will present a perspective on how to integrate findings from both methods to advance EDL models in the future. Adequately fine-tuned EDL models for specific electrochemical conditions will provide valuable structural information, which can then be compared with recent experimental findings [16, 17], and yield properties to compare with experimentally obtained interface parameters and response functions such as the potential of zero charge (pzc) and the double layer capacitance [18, 19].

II. SEMICLASSICAL DENSITY-POTENTIAL FUNCTIONAL THEORY

TABLE I. Comparison between AIMD +implicit solvent and semiclassical methods. The semiclassical and AIMD+implicit solvent approaches combine theories on different scales for the electrode and electrolyte, while AIMD simulations treat all parts on a same level.

	AIMD (+implicit)	Semi-classical
Scale	Microscopic	Multiscale
Ensembles	Canonical NVT	Grand canonical μVT
Constraints	N_{el}	μ_{el}, pH, $\cdots$
Sampling time	< 100 ps	Static
System size	$< 10^3$ atoms	N_A particles
Computer time	$\sim$1M CPU hours	Several minutes for 1D model
Statistical average $\langle A \rangle =$	$\frac{1}{T}\int_{t=0}^{T} A(\{R\}, n; t)dt$	$\mathcal{A}$
Electrode potential U	Work function $\Phi(t)$	Electron chemical potential μ_{el}
Electric potential $\phi(z)$	$\int_A \phi(r,t)dxdy/A$	Inner potential $\varphi(z)$
Structural factors	Atomic coordinates $\{R(t)\}$	Adjustable parameters
	(Local permittivity $\epsilon(z,t)$)	Gap t, ionic cores a_{mc}, $\cdots$

A computationally feasible and insightful approach to treat the EDL within a grand-canonical scheme is the semiclassical EDL model by Huang et al. It combines an orbital-free quantum-mechanical description of the electrode and a classical statistical field description

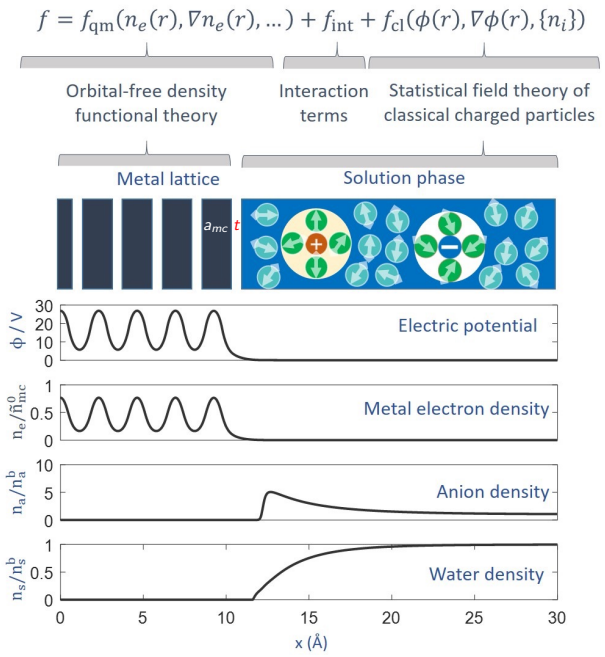

FIG. 1. A hybrid density-potential functional theory for the EDL. The EDL is divided into an inhomogeneous electron gas described by quantum mechanical DFT, and an inhomogeneous Coulombic fluid described by classical statistical field theory. This model is different from the joint DFT model developed by Arias et al. on two aspects [20, 21]. Firstly, orbital-free DFT is used and the electron density distribution is solved from a Euler-Lagrange equation with negligible computational cost. Therefore, this model capable of simulating realistic EDLs. Secondly, a hybrid DPFT is developed to describe the electrolyte solution considering asymmetric steric effects, solvent polarization, and ion-specific interactions with the metal. These factors are not considered in the variants of Poisson-Boltzmann theory used in joint DFT. Subplots in the figure show the distributions of the electric potential, the metal electron density normalized to the electron density of the metal cationic cores, the anion density and the water molecule density, both normalized to their bulk values, from the metal phase to the solution phase [8].

of the electrolyte, as sketched in Fig. 1 [7–9]. The electrode is assumed to consist of a one-dimensional array of layers. The width of these layers is assumed to correspond to the core radius a_{mc} of metal cations. Furthermore, a spacing t between the metal electrode and water is assumed. These two parameters are typically derived from DFT calculations. For simplicity, atomic cores are represented by a constant positive charge. In the present variant,

the kinetic and exchange-correlation energies of electrons are addressed by the Thomas-Fermi-von Weizsäcker and Dirac-Wigner theories, respectively. Classical density-potential functional theory (DPFT) describes the electrolyte solution accounting for the asymmetric steric effects and solvent polarization in the electrolyte solution and ion-specific interactions of electrolyte species with the electrode [9].

The grand potential of the whole EDL includes the electrode, electrolyte, and the interactions between them. Variational analysis of the grand potential yields a grand-canonical picture of the EDL using two Euler-Lagrange equations in terms of the electron density and the electric potential. Avoiding the Kohn-Sham orbital optimization, the computational cost of this approach becomes negligible compared with Kohn-Sham DFT-based methods, such as the joint DFT developed by the Arias and coworkers [20, 21].

The semiclassical method provides a computationally efficient description of EDL properties within a grand-canonical scheme, i.e., it describes the electrode and the electrolyte solution on equal footing. Figure 1 shows the EDL properties determined under constant potential conditions, which include the oscillating electron density in the metal lattice, electron spillover from the electrode, accumulation (depletion) of counterions (coions) in the diffuse layer, the field-dependent orientation of solvent molecules, and partial charge transfer, if any, described with an Anderson-Newns type model [8].

However, the presented orbital-free DFT is a crude approximation [22, 23], and its accuracy in an electrochemical environment is still unknown. The chemical interaction between ions/molecules in solution and the electrode, which is essential for chemisorption and more complicated electrocatalytic phenomena, requires further attention. In addition, the semiclassical model is currently unable to optimize the structure of the EDL. Most importantly, it introduces a structural parameter, the gap between the species (solvent molecules and ions) in the electrolyte and cationic cores in the electrode, which determines all the important EDL properties. For example, stronger specific ion adsorption could result in a smaller gap t between the electrode and electrolyte, and it causes a smaller pzc and an elevated double-layer capacitance curve [8].

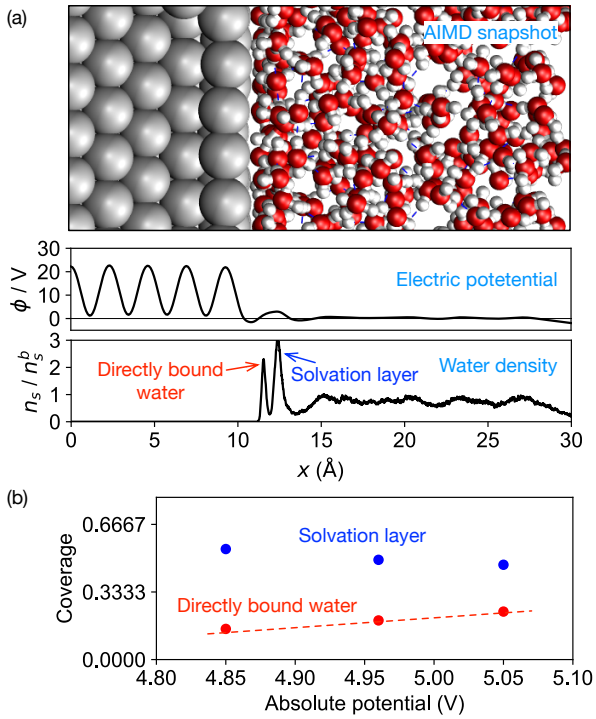

FIG. 2. (a) AIMD simulations of the interface between Pt(111) and water at the pzc. The unit cell consists of 612 atoms and 2952 electrons. The statistical average has performed over 40 ps by solving Langevin equation at 293 K [4, 24]. (b) The coverage of solvating water molecules as a function of the electrode potential [24].

III. AIMD SIMULATIONS

DFT calculations yield the total energy, the electron density distribution, and the forces acting on atoms upon solving the Kohn-Sham equation. The EDL properties can then be statistically determined by molecular dynamics simulations using the ergodic theorem. Kohn-Sham DFT is known to describe metal-metal, metal-adsorbate, and water-water interactions with high reliability [11, 25], but it is computationally more demanding compared to orbital-free DFT. A typical electrochemical property that can be determined by AIMD simulations in good agreement with the experiment [18, 19] is the potential of zero charge [3, 4, 10, 12], which can be derived from the work function of an ion-free water film above a metal slab [26], as illustrated in Fig. 2. It is nonetheless necessary to be aware of possible shortcomings of DFT approaches due to the approximate nature of the employed functionals. In particular, water-water and water-metal interaction cannot properly be de-

scribed without adequate consideration of van der Waals interactions [11, 15].

However, due to their high computational demand, AIMD simulations in the canonical ensemble can only consider relatively small systems for limited run times typically below 100 ps (see Table I). The representation of electrified interfaces poses a particular challenge. In periodic calculations, the unit cell has to be electrostatically neutral, and any surplus charge is automatically compensated by a homogeneous charge background. In principle, electrochemical interfaces also have to be charge-neutral, and any excess charge in the electrolyte will be balanced by the corresponding countercharge on the metal electrode. Within the framework of DFT, there are two approaches to reproduce the compensating polarization. An appropriate EDL configuration can be tailored using explicit ions. In practice, by adding a charge-neutral atom of a target ion into the water film, the electrons of the atom are transferred to the Fermi level of the electrode, and this electron exchange between the electrode and atom species on the electrolyte side creates ionic species in the water film [4, 27–29]. Otherwise, the compensating polarization in the electrolyte can be implicitly modeled by the Boltzmann distribution. The net polarization distribution is optimized with the electron density by simultaneously solving the Kohn-Sham and the linearized Poisson-Boltzmann equations [20, 30–32].

IV. BRIDGING AIMD AND SEMICLASSICAL METHODS

After briefly discussing the strengths and weaknesses of both the semiclassical method and the AIMD approaches, we will now consider how these two approaches can be interconnected. Semiclassical approaches can describe the EDL within a grand-canonical scheme, whereas AIMD simulations can provide atomistic details of the interface. The atomic configurations presenting polarization effects identified in AIMD simulations can be used as input for the improved parametrization of the semiclassical method. Conversely, the semiclassical method can guide preparing and validating the atomic setup in AIMD simulations.

One of the factors determining polarization effects at the interface is the particular configuration of water that is statistically sampled along the AIMD trajectories to calculate effective water properties. As demonstrated with early simulations employing an ice-like bilayer model on close-packed metal surfaces [33], separately treating charge species in electrode and electrolyte and relying only on the orientation of the O-H bonds are insufficient

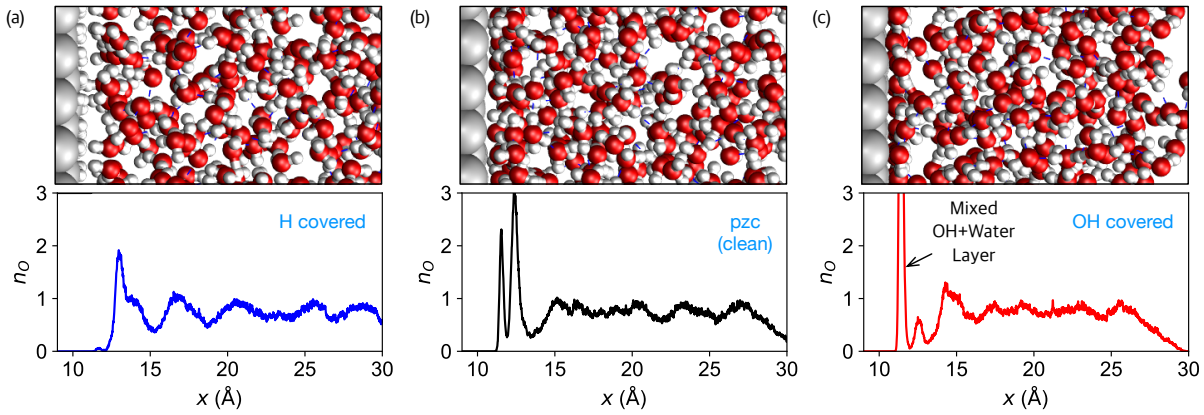

FIG. 3. O atom distribution in the water films on (a) H covered, (b) clean, and (c) OH covered Pt(111) electrodes. On H covered electrode, no directly bound water molecules are found, whereas the directly bound water and OH molecules form a compact solvation layer on OH covered electrode [4, 24].

to capture the formation of the interface dipole, especially on transition metals. The charge analysis shows that a considerable amount of electron transfer occurs between water layer and metal, contributing to the interface dipole field. These findings were confirmed by the analysis of AIMD simulations using several water layers on metal surfaces [3, 4, 6]. In addition to the water orientation, they identified a densely packed water solvation layer with a strong electronic charge redistribution contributing to the interfacial polarization field.

In a recent detailed study, Li et al. [10] found that the strong bonding of the water molecules to the surface (see Fig. 2a) weakens one of the O-H bonds, which supports the formation of Hydronium or Zundel configurations from water molecules on transition metal surfaces [4, 5, 10, 12, 13]. Polarization of interfacial liquid water also exist at the pzc, i.e., without adding ionic species. As Le et al. showed [5], the weakened O-H bonds are associated with a redshift of the O-H stretch vibration that facilitates the proton motion at the interface through the structural diffusion, which causes a higher proton activity at the interface than in bulk liquid water. Furthermore, Lan et al. showed that nuclear quantum effects could further enhance the proton activity in the solvation layer [13].

The water configurations encountered at the interface determine the relative potential difference between bulk liquid water to the electrode phases. As demonstrated by recent AIMD simulations, the electric potential in the bulk water potential is placed much closer

to the Fermi level when the electrolyte is explicitly modeled by water molecules, compared to an implicit solvent [34, 35]. Without the explicit consideration of water configurations at the interface, i.e., neglecting directly bound water molecules, the implicit solvent method does not account for charge transfer at the interface and therefore underestimates the impact of interface. As identified by Li et al. [10], the Helmholtz model can capture the polarization properties of the strongly bound water molecules. The specific water configuration equivalent to the formation of a Helmholtz layer is only stable when the metal-water interaction is strong enough, like on transition metal electrodes. On noble metal electrodes like Ag and Au, where the metal-water interaction is weak, the formation of such a water configuration is less pronounced. The corresponding semiclassical assessment requires the gap parameter t [8, 36], which is related to the distance to the Helmholtz layer. The parameter t also needs to reflect the interaction strength between metal and water and further considerations than the cation spacing.

One of the OH bonds of most water molecules points toward the electrode on Pt(111). Charging up the electrode by populating the water film with ionic species leads to a linear relationship between the coverage of directly bound water molecules to the electrode and the work function. As shown in Fig. 2b, there is an exchange between directly bound water molecules (red dots) and solvating molecules with pointing the OH toward the electrode (blue dots) by varying the electrode charging. The increase of the number of directly bound water molecules is in line with the increase of the interface dipole.

Since the structural change in the solvation layer is a response to the field created by the electrolyte polarization [20, 31, 32, 37, 38], it is not trivial to faithfully reproduce this effect in the parametrization of implicit solvent methods through the solvation cavity and local permittivity at the contact [39]. There are advanced approaches to address the solvation structures without relying on the cavity, namely the reference interaction site method (RISM) [40, 41], but the delicate structures of the solvation layer in Fig. 3 are still challenging to be captured within the approach.

The adsorbed species also change the polarization at the interface [4, 10, 42–45]. When adsorbate-metal interactions are stronger than water-metal interactions, then the adsorbates effectively replace water molecules at the interface. For example, the H adsorption blocks the direct adsorption of water molecules and increases the distance between the solvating water molecules and the electrode by around 1 Å at low potentials, as shown in Fig. 3. The

increased distance between the water molecules and the surface weakens their interaction. When anionic species cover the electrode, e.g., OH^- [46–48], they alter the solvation layer structure significantly. As recently demonstrated [49, 50], adsorbed sulfate (SO_4^{2-}) interacts strongly with the water molecules and forms a stable mixed water-sulfate layer on Au and Pt electrodes. The stable anionic species significantly contribute to the interface dipole. A mixed water-OH^- layer configuration at high electrode potential [51] has been found by Zhu et al. [48]. The solvating water structures become strongly modified at the interface, and again the stable anionic species significantly contribute to the interface dipole.

The competition between water molecules and ion species in the solvation layer can be realized by a constraint of the molecule density within the semiclassical method [39]. In the semiclassical model, the competing behavior between water molecules and ions is determined by the respective electrochemical potentials, which are derived from the grand potential of the EDL. The competition is codetermined by electrostatic, hard-sphere, and electronic interactions.

Although DFT can reproduce the interface structure with high reliability, the models must be adequately prepared for specific electrochemical environments. When an atomic configuration does not match the considered condition and fails to reproduce the experimental situation, the results might be irrelevant for the assumed environment. For example, within AIMD simulations, the relation between the interface dipole and the adsorbate-induced change of the water/electrode interaction seems opposite to the potential change. A more negatively polarized electrode requires a higher concentration of directly adsorbed water molecules blocked on the hydrogen-covered electrode. The charge in the Helmholtz layer created by the water molecules strongly bound to the electrode depends on the coverage of the corresponding water species. A higher H coverage causes an increase of the work function [10], which does not match the supposed electrochemical condition, i.e., H coverage at a low electrode potential. Adequate modeling requires simultaneous consideration of the ion distribution in the electrolyte and adsorbates for a condition [44]. It has to be realized that AIMD simulations, due to their high computational demand, are not the right method to yield information about the optimal adsorbate coverage and ion distribution together. Here calculations based on the semiclassical method can provide valuable information that then enters the choice of the initial configurations entering the AIMD simulations.

V. CONCLUSION

We have sketched the recent progress in the theoretical and numerical determination of EDL structures at electrode/electrolyte interfaces from AIMD and semiclassical approaches. Despite this recent progress, the research field requires further progress. In AIMD simulations, a proper setup of atomic configurations which are suitable to represent the desired electrochemical environments is essential. Because of the high computational demand of AIMD simulations, the selection of their initial configuration should be based on preceding grand-canonical treatment. Thus, an important role of semiclassical approaches might be to provide valuable initial input for AIMD simulations. Still, the semiclassical model can also be further improved with respect to a better description of the electronic structures of the electrode, a more reliable representation of ion/molecule bonds, a beyond-mean-field treatment of the electrolyte, and the coupling with micro-kinetic models. These systematic improvements should be closely based on quantum chemical arguments, including input from AIMD simulations.

DECLARE OF INTEREST

Declare of interest: none.

ACKNOWLEDGEMENT

This research has been supported by the German Research Foundation (DFG) through contract GR 1503/39-1, the Alexander von Humboldt Foundation, and National Natural Science Foundation of China under the grant number of 21802170. Computer time provided by the bwHPC initiative and the bwHPC-C5 project funded by the Baden-Württemberg government (MWK) and the German Research Foundation (DFG) through grant number INST 40/575-1 FUGG (JUSTUS 2 cluster) is gratefully acknowledged. This work contributes to the research performed at CELEST (Center for Electrochemical Energy Storage Ulm-Karlsruhe).

REFERENCES

· Paper of special interest

·· Paper of outstanding interest

---

[1] W. Schmickler, Chem. Rev. **96**, 3177 (1996).

[2] A. Groß and S. Sakong, Curr. Opin. Electrochem. **14**, 1 (2019).

[3] J. Le, M. Iannuzzi, A. Cuesta, and J. Cheng, Phys. Rev. Lett. **119**, 016801 (2017).

[4] S. Sakong and A. Groß, J. Chem. Phys. **149**, 084705 (2018).

[5] J. Le, Q. Fan, L. Perez-Martinez, A. Cuesta, and J. Cheng, Phys. Chem. Chem. Phys. **20**, 11554 (2018).

[6] J.-B. Le and J. Cheng, Curr. Opin. Electrochem. **19**, 129 (2020).

[7] J. Huang, P. Li, and S. Chen, Phys. Rev. B **101**, 125422 (2020).

[8] J. Huang, S. Chen, and M. Eikerling, J. Chem. Theory Comput. **17**, 2417 (2021).

·· This paper presents a semiclassical framework to address the grand potential of the EDL by combining an orbital-free quantum mechanical method and classical density-potential functional theory. The method treats the whole EDL on the same footing.

[9] J. Huang, Electrochim. Acta **389**, 138720 (2021).

[10] P. Li, J. Huang, Y. Hu, and S. Chen, J. Phys. Chem. C **125**, 3972 (2021).

·· This AIMD study identifies the origin of the interface dipole at the water/Pt(111) interface and connects to a specific water configuration. Furthermore, it addresses the influence of H coverage on the dipole strength.

[11] S. Sakong, K. Forster-Tonigold, and A. Groß, J. Chem. Phys. **144**, 194701 (2016).

[12] J. Le, A. Cuesta, and J. Cheng, J. Electroanal. Chem. **819**, 87 (2018).

[13] J. Lan, V. V. Rybkin, and M. Iannuzzi, J. Phys. Chem. Lett. **11**, 3724 (2020).

· This AIMD study discusses the proton activity at the water/Pt(111) interface also regarding the nuclear quantum effects.

[14] C. K. Jung, L. Braunwarth, and T. Jacob, J. Chem. Theory Comput. **15**, 5810 (2019).

[15] S. K. Natarajan and J. Behler, Phys. Chem. Chem. Phys. **18**, 28704 (2016).

[16] E. H. G. Backus, J. Schaefer, and M. Bonn, Angew. Chem. Int. Ed. **60**, 10482 (2020).

[17] Y.-H. Wang, S. Zheng, W.-M. Yang, R.-Y. Zhou, Q.-F. He, P. Radjenovic, J.-C. Dong, S. Li, J. Zheng, Z.-L. Yang, G. Attard, F. Pan, Z.-Q. Tian, and J.-F. Li, Nature **600**, 81 (2021).

[18] N. Garcia-Araez, V. Climent, and J. Feliu, J. Phys. Chem. C **113**, 9290 (2009).

[19] V. Briega-Martos, E. Herrero, and J. M. Feliu, Curr. Opin. Electrochem. **17**, 97 (2019).

[20] K. Letchworth-Weaver and T. A. Arias, Phys. Rev. B **86**, 075140 (2012).

[21] R. Sundararaman, W. A. Goddard, and T. A. Arias, J. Chem. Phys. **146**, 114104 (2017).

[22] Y. A. Wang and E. A. Carter, *Orbital-free Kinetic-energy Density Functional Theory* (Springer, 2002), chap. 5, pp. 117–184, ISBN 978-0-306-46949-7.

[23] V. Gavini, K. Bhattacharya, and M. Ortiz, J. Mech. Phys. Solids **55**, 697 (2007).

[24] S. Sakong and A. Groß, Phys. Chem. Chem. Phys. **22**, 10431 (2020).

[25] D. Mahlberg, S. Sakong, K. Forster-Tonigold, and A. Groß, J. Chem. Theory Comput. **15**, 3250 (2019).

[26] S. Trasatti, Electrochim. Acta **36**, 1659 (1991).

[27] E. Skúlason, G. S. Karlberg, J. Rossmeisl, T. Bligaard, J. Greeley, H. Jónsson, and J. K. Nørskov, Phys. Chem. Chem. Phys. **9**, 3241 (2007).

[28] J.-B. Le, Q.-Y. Fan, J.-Q. Li, and J. Cheng, Sci. Adv. **6**, eabb1219 (2020).

[29] J.-B. Le and J. Cheng, Curr. Opin. Electrochem. **27**, 100693 (2021).

[30] M. Otani and O. Sugino, Phys. Rev. B **73**, 115407 (2006).

[31] M. M. Melander, M. J. Kuisma, T. E. K. Christensen, and K. Honkala, J. Chem. Phys. **150**, 041706 (2019).

[32] K. Mathew, V. S. C. Kolluru, S. Mula, S. N. Steinmann, and R. G. Hennig, J. Chem. Phys. **151**, 234101 (2019).

[33] S. Schnur and A. Groß, New J. Phys. **11**, 125003 (2009).

[34] N. G. Hörmann, Z. Guo, F. Ambrosio, O. Andreussi, A. Pasquarello, and N. Marzari, Npj Comput. Mater. **5**, 100 (2019).

[35] G. Bramley, M.-T. Nguyen, V.-A. Glezakou, R. Rousseau, and C.-K. Skylaris, J. Chem. Theory Comput. **16**, 2703 (2020).

[36] J. Liu and J. Huang, J. Electroanal. Chem. **846**, 113136 (2019).

[37] J.-L. Fattebert and F. Gygi, J. Comput. Chem. **23**, 662 (2002).

[38] K. Mathew, R. Sundararaman, K. Letchworth-Weaver, T. A. Arias, and R. G. Hennig, J. Chem. Phys. **140**, 084106 (2014).

[39] E. Gongadze and A. Iglič, Bioelectrochemistry **87**, 199 (2012).

[40] J. Haruyama, T. Ikeshoji, and M. Otani, Phys. Rev. Materials **2**, 095801 (2018).

[41] R. Tesch, P. M. Kowalski, and M. H. Eikerling, J. Phys.: Condens. Matter **33**, 444004 (2021).

[42] M. H. Hansen, A. Nilsson, and J. Rossmeisl, Phys. Chem. Chem. Phys. **19**, 23505 (2017).

[43] R. Kronberg and K. Laasonen, J. Phys. Chem. C **124**, 13706 (2020).

[44] J.-B. Le, A. Chen, L. Li, J.-F. Xiong, J. Lan, Y.-P. Liu, M. Iannuzzi, and J. Cheng, JACS Au **1**, 569 (2021).

· This paper addresses tailoring the surface coverage and ions in the electrolyte simultaneously to match an electrochemical condition.

[45] S. Surendralal, M. Todorova, and J. Neugebauer, Phys. Rev. Lett. **126**, 166802 (2021).

[46] H. H. Kristoffersen, T. Vegge, and H. A. Hansen, Chem. Sci. **9**, 6912 (2018).

[47] H. H. Kristoffersen, K. Chan, T. Vegge, and H. A. Hansen, Chem. Commun. **56**, 427 (2020).

[48] J.-X. Zhu, J.-B. Le, M. T. M. Koper, K. Doblhoff-Dier, and J. Cheng, J. Phys. Chem. C **125**, 21571 (2021).

[49] F. Gossenberger, F. Juarez, and A. Groß, Front. Chem. **8**, 634 (2020).

[50] Y. Fang, S.-Y. Ding, M. Zhang, S. N. Steinmann, R. Hu, B.-W. Mao, J. M. Feliu, and Z.-Q. Tian, J. Am. Chem. Soc. **142**, 9439 (2020).

[51] S. Sakong, D. Mahlberg, T. Roman, M. Li, M. Pandey, and A. Groß, J. Phys. Chem. C **124**, 27604 (2020).